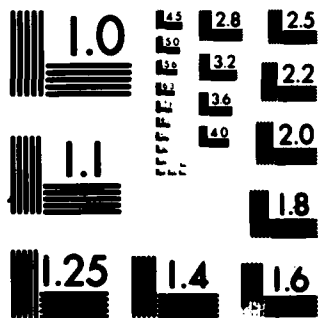END
DATE
FILMED

4-81

DTIC

MICROCOPY RESOLUTION TEST CHART

NATIONAL BUREAU OF STANDARDS-1963-A

Large-Diameter CO_2 Laser Facility for Testing Optical Resonators

Prepared by

E. B. TURNER and R. A. CHODZKO
Aerophysics Laboratory
Laboratory Operations
The Aerospace Corporation
El Segundo, Calif. 90245

29 September 1980

Interim Report
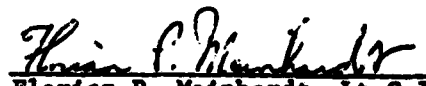
This interim report was submitted by The Aerospace Corporation, El Segundo, CA 90245, under Contract No. F04701-79-C-0080 with the Space Division, Deputy for Technology, P.O. Box 92960, Worldway Postal Center, Los Angeles, CA 90009. It was reviewed and approved for The Aerospace Corporation by W. R. Warren, Jr., Director, Aerophysics Laboratory.
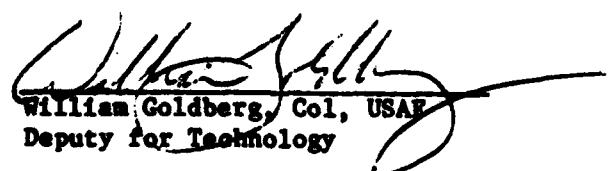
This report has been reviewed by the Public Affairs Office (PAS) and is releasable to the National Technical Information Service (NTIS). At NTIS, it will be available to the general public, including foreign nations.

This technical report has been reviewed and is approved for publication. Publication of this report does not constitute Air Force approval of the report's findings or conclusions. It is published only for the exchange and stimulation of ideas.

James C. Garcia, 1st Lt, USAF
Project Officer

Florian P. Meinhardt, Lt Col, USAF
Director, Directorate of Advanced
    Space Development

FOR THE COMMANDER

William Goldberg, Col, USAF
Deputy for Technology

REPORT DOCUMENTATION PAGE

READ INSTRUCTIONS
BEFORE COMPLETING FORM

1. REPORT NUMBER	2. GOVT ACCESSION NO.	3. RECIPIENT'S CATALOG NUMBER
SD-TR-80-89	AD-A096 267	

4. TITLE (and Subtitle)	5. TYPE OF REPORT & PERIOD COVERED
LARGE-DIAMETER CO$_2$ LASER FACILITY FOR TESTING OPTICAL RESONATORS.	Interim rept.,
	6. PERFORMING ORG. REPORT NUMBER
	TR-0080(5605)-2

7. AUTHOR(s)	8. CONTRACT OR GRANT NUMBER(s)
Eugene B. Turner and Richard A. Chodzko	F04701-79-C-0080

9. PERFORMING ORGANIZATION NAME AND ADDRESS	10. PROGRAM ELEMENT, PROJECT, TASK AREA & WORK UNIT NUMBERS
The Aerospace Corporation El Segundo, Calif. 90245	

11. CONTROLLING OFFICE NAME AND ADDRESS	12. REPORT DATE
Air Force Weapons Laboratory Kirtland Air Force Base, N. Mex. 87117	29 September 1980
	13. NUMBER OF PAGES
	41

14. MONITORING AGENCY NAME & ADDRESS(if different from Controlling Office)	15. SECURITY CLASS. (of this report)
Space Division Air Force Systems Command Los Angeles, Calif. 90009	Unclassified
	15a. DECLASSIFICATION/DOWNGRADING SCHEDULE

16. DISTRIBUTION STATEMENT (of this Report)

Approved for public release; distribution unlimited.

17. DISTRIBUTION STATEMENT (of the abstract entered in Block 20, if different from Report)

18. SUPPLEMENTARY NOTES

19. KEY WORDS (Continue on reverse side if necessary and identify by block number)

Annular Laser Resonators
Closed-Cycle Gas Flow System
CO$_2$ Laser
Large Equivalent Fresnel Number

Optical Resonator Test Facility
Repetitively Pulsed Electrical Discharge
Unstable Laser Resonators

20. ABSTRACT (Continue on reverse side if necessary and identify by block number)

A closed-cycle CO$_2$ laser facility with a clear aperture diameter of 18.7 cm was developed for testing large diameter optical resonators designed for use with cylindrical chemical lasers that have an annular gain region.

In this report, the considerations that lead to the present laser facility design are discussed, and the results of the open-cycle tests that established the feasibility of the design are presented. The closed-cycle gas flow system and

DD FORM 1473
(FACSIMILE)

19. KEY WORDS (Continued)

20. ABSTRACT (Continued)

the high-voltage electrical discharge circuits are described, the operating parameters are given, and the results of some gas flow and electrical discharge measurements are presented. The performance of the facility was established by gain measurements and by the beam quality obtained with several resonators.

PREFACE

The authors thank Stephen B. Mason for assisting with the open-cycle CO_2 laser experiments and Marquis E. Gerard for his help in assembling and testing the closed-cycle system. The authors also thank Donald A. Durran for his contributions to the design of the flow manifolds and for his assistance and advice on the design and test of the refrigeration cooling system and Wilbur A. Garber for his design of the grid pulser circuit. Finally, the authors wish to acknowledge the support given them by their supervisor Harold Mirels and by Maj. William Plummer, the project officer of the Air Force Weapons Laboratory.

Accession For

NTIS GRA&I ☑
TAB ☐
announced ☐
fication

ility Codes

and/or
Special

A

1

CONTENTS

FIGURES

TABLES

I. INTRODUCTION

The resonators proposed for use with cylindrical chemical lasers are usually half-symmetric unstable resonators with axicon mirrors that transform an annular cross section into a circular compacted area. A typical resonator of this type, called a linear half-symmetric unstable resonator with internal axicon (HSURIA), is shown in Fig. 1. Data are desired on various aspects of this resonator, including mode control, beam quality, sensitivity to misalignment of the optical elements, polarization of the beam, effect of support struts, and obscuration of the W-axicon tip. These data will be used to determine the acceptability of various resonator configurations proposed for use with the cylindrical chemical lasers. The CO_2 laser facility designed for obtaining these data has been in operation since early 1978 and has been responsible for some significant results on polarization effects associated with HSURIAs, which have been published recently.[1]

The requirements and constraints imposed on the facility design are described in Section II. In Section III, a brief summary is given of the open-cycle tests that established the feasibility and defined the range of operating parameters for the closed-cycle CO_2 laser facility. The gas flow system, the flow parameters, and the results of some gas flow measurements are discussed in Section IV. A description of the high-voltage electrical discharge circuits, together with some measurements of the gas discharge, is presented in Section V. The system performance as determined by gain measurements, interferometric analysis of medium homogeneity, and beam quality of several HSURIAs, is discussed in Section VI. The report is then concluded with a brief summary and some general comments.

---

[1] R.A. Chodzko, S.B. Mason, and E.B. Turner, Appl. Opt. 19, 778 (1980).
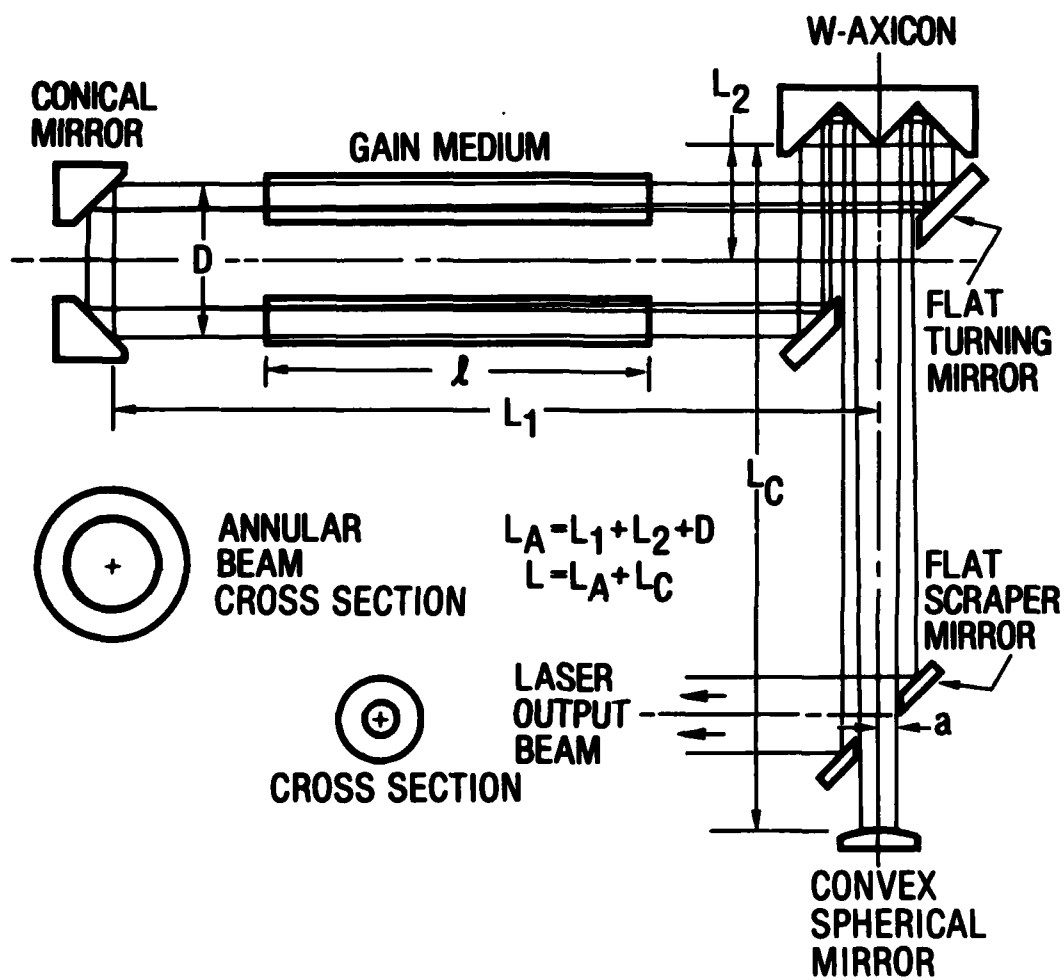
9

Fig. 1. Linear HSURIA Laser

II. DESIGN CONSIDERATIONS

A repetitively pulsed, closed-cycle CO_2 laser design was selected for
several reasons. First, the relatively long wavelength of a CO_2 laser
(10.6 μm) was preferred so that the laser wavelength would be much larger than
the figure errors (approximately ±1 μm) of the diamond-turned metal mirrors to
be used in resonator tests. Second, there was a good technology base for CO_2
electrical discharge lasers. A repetitively pulsed CO_2 laser with a 4-in. di-
ameter had been built and operated successfully at the Air Force Weapons Labo-
ratory. Third, it was desirable that the laser operate continuously for long
periods of time so that the effects of mirror adjustments could be observed in
real time and measured. It was, however, necessary to keep the average power
low to minimize thermal distortion of the mirrors. Because of these issues,
the use of a continuous-flowing, repetitively pulsed device was indicated.
The expenditure of gas is prohibitive for an open-cycle system, so a closed-
cycle system was planned.

The window diameter of 19.7 cm was ultimately determined by the cost and
availability of the ZnSe window material. The equivalent Fresnel number, how-
ever, had to be at least 4.5 to provide a reasonably good simulation of the
resonator and annular gain medium of a large cylindrical chemical laser. The
equivalent Fresnel number of a half-symmetric unstable resonator is defined by

$$N_{eq} = \frac{a^2}{2\lambda L} \frac{(M^2 - 1)}{2M}$$

where M is the resonator magnification, L is the cavity length, λ is the
lasing wavelength, and a is the radius of the hole in the output coupling
mirror. These dimensions are shown in Fig. 1.

In Fig. 2, the maximum equivalent Fresnel number that can be obtained for
the clear aperture diameter of 18.7 cm is plotted versus L_c, the compacted
beam length. The Fresnel number is plotted for two typical values of magni-
fication, M = 1.5 and M = 2.0, and for two values of gain medium length,

11
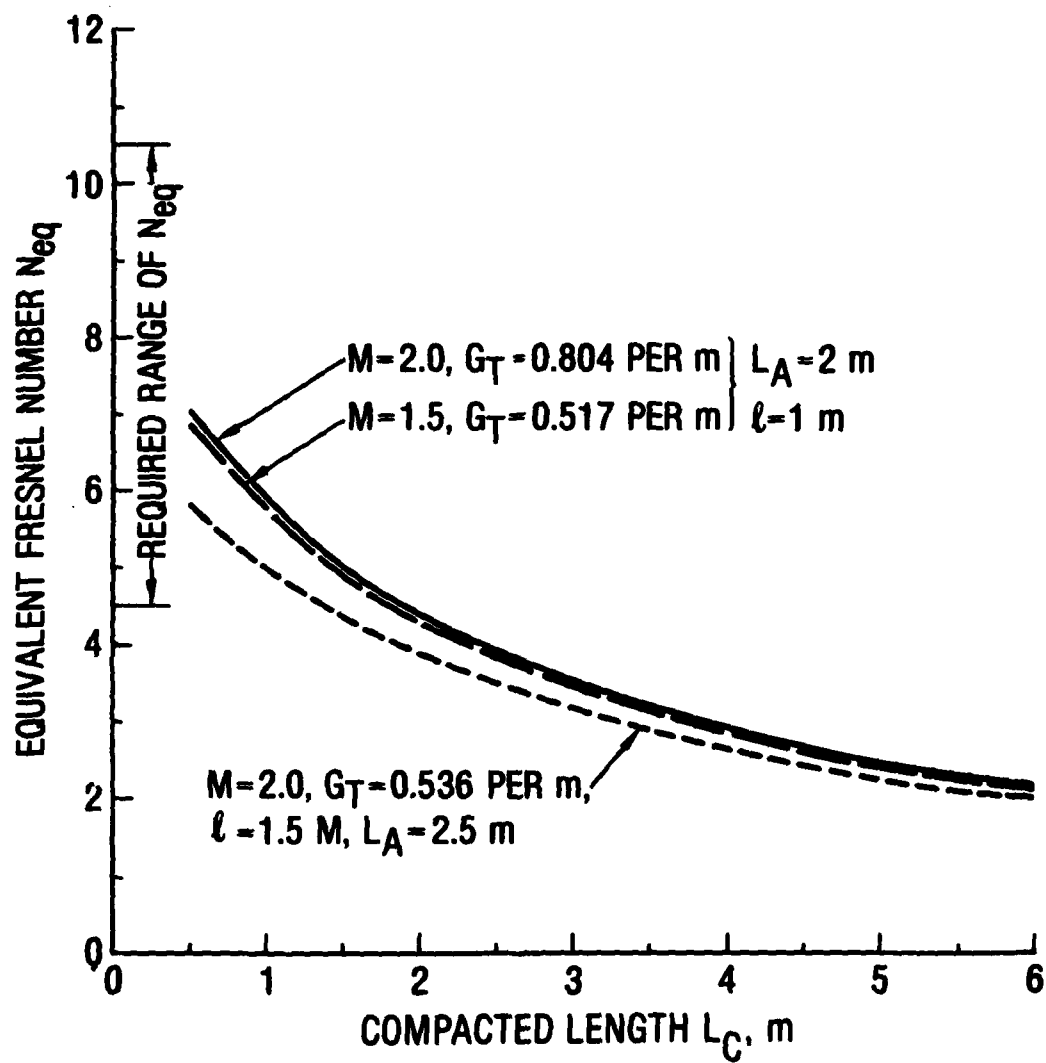
Fig. 2. Curves of N_{eq} Versus L_C for the HSURIA

$\ell = 1.0$ and $\ell = 1.5$ m. The effective length of the annular leg must be about 1.0 m longer than the length of the gain medium to permit space for gas manifolds and optical mounts. The total cavity length L is the sum of L_C and L_A.

The threshold gain, also indicated for each curve in Fig. 2, is given by

$$G_T = \frac{1}{2\ell} \ln \frac{M^2}{0.80}$$

which is valid in the geometric optics limit. The value 0.80 is an estimate of the total mirror reflectivity and window transmission for one round trip of the resonator. It can be seen from the graph that the equivalent Fresnel number is higher for the shorter length of the gain region ℓ, but that the threshold gain is also higher. A tentative decision was made to limit the length of the discharge tube to 1 m, which made it necessary to achieve a medium gain of somewhat greater than 0.804/m, the threshold value for M = 2.0.

In addition to the requirements just discussed, it was necessary that the electrical discharge be homogeneous with no arc streamers. Also, it was required that the gas flow or discharge not introduce appreciable inhomogeneities in the refractive index of the medium that might degrade the beam quality.

III. OPEN-CYCLE TESTS

The feasibility of the large-diameter electrical discharge laser was first established and the operating conditions of the laser were determined by an open-cycle test facility before the closed-cycle system was designed.

An existing large-capacity vacuum pumping system was used to provide volumetric flow rates of up to 10,000 cfm at pressures of up to 10 Torr. A 60-gal mixing tank filled to 200 psi provided sufficient gas for run times of a few minutes per filling depending on the gas flow rate. The gas flow rate was adjusted by setting the pressure upstream of a sonic metering orifice, and the discharge tube pressure was adjusted with the use of a large ball valve to the vacuum pumping system. The electrical discharge took place in a 22-cm-i.d. glass pipe located between two rings that consisted of 12 electrodes each, which were spaced 127 cm apart. Observations were made on the homogeneity of the electrical discharge and on the gain of the medium for a range of gas pressures and mixtures, gas flow velocities, pulse current amplitudes and duration, and glow discharge currents.

It was found that uniform electrical discharges could be obtained at gas pressures of up to 4 Torr with pulse currents of about 6 A and pulse durations of 1 ms in a gas mixture of 1:1:4 of $CO_2:N_2:He$, with the use of a continuous-wave (cw) glow discharge current of 60 mA and a gas flow rate of over 2000 cfm. Arc streamers would form for slower volumetric flow rates or for mixtures with less helium. The measured gain was fairly uniform across the tube and was 1.3/m for the parameters just given, which was well above the threshold value (Fig. 2).

IV. CLOSED-CYCLE FLOW SYSTEM

A. FUNCTIONAL DESCRIPTION

A large Roots vacuum pump was used in the closed-cycle facility to circulate the gas continuously through the system. Figure 3 is a schematic diagram of the flow system. The flow enters the aluminum inlet manifold at a pressure of about 4.6 times the operating pressure in the discharge tube. The gas then flows radially inward through a series of 50 sonic orifices around the inner circumference of the manifold. The pressure is thereby dropped to the proper operating pressure in the discharge tube. The gas exits through an aluminum output manifold and continues to the inlet of the Roots pump where it is compressed. A small amount of the gas (about 1%) is removed during each round trip by an auxiliary 50-cfm mechanical pump. This gas is replaced by a small flow from the gas supply-mixing tank, which minimizes the buildup of contaminants in the lasing gas.

It is necessary to cool the gas with Freon heat exchangers. The first cooler, which is located at the inlet to the Roots pump, removes the heat of the electrical discharge. The second cooler (actually two coolers in series) is used to remove the heat of compression at the exit of the Roots pump. A final cooler is placed at the exit of the plenum chamber. The coolers work very well even at the low pressure of 4 to 16 Torr because of the high thermal conductivity of the helium gas. A long glass pipe is used on the inlet side of the discharge tube to prevent the discharge from going backwards toward the plenum chamber. The high-voltage anodes are on the upstream side of the discharge tube so that the ions drift with the gas flow.

Figure 4 is a photograph of the completed closed-cycle CO_2 laser facility. The large Newport Research Corporation vibration-isolated optical table is in the foreground. The discharge tube is suspended over the table by means of a cantilever support, and it does not touch the table. The glass pipe is supported by a Unistrut steel framework. The high-voltage power supply and high-voltage circuit rack, with the current pulser, are at the left of the photograph. Figure 5 is a photograph of the rear view of the facility. The
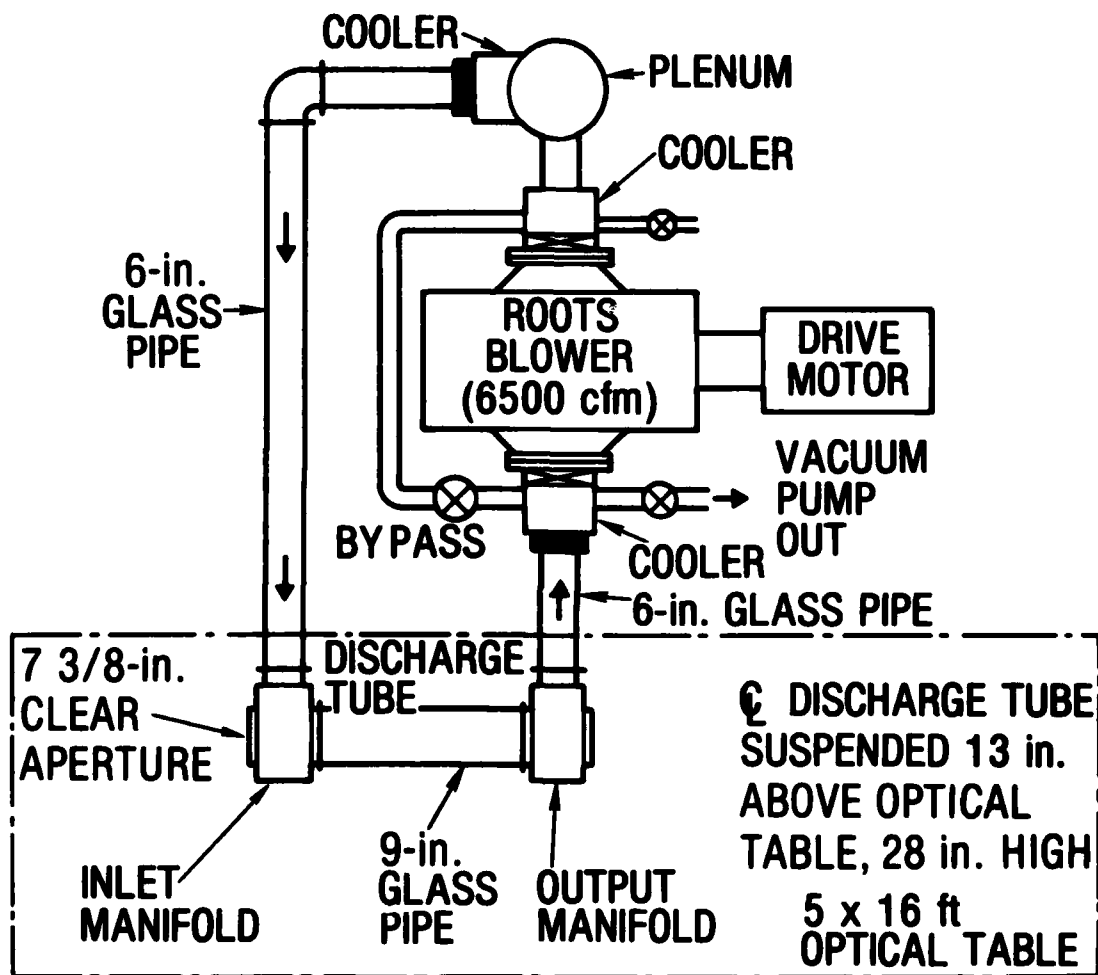
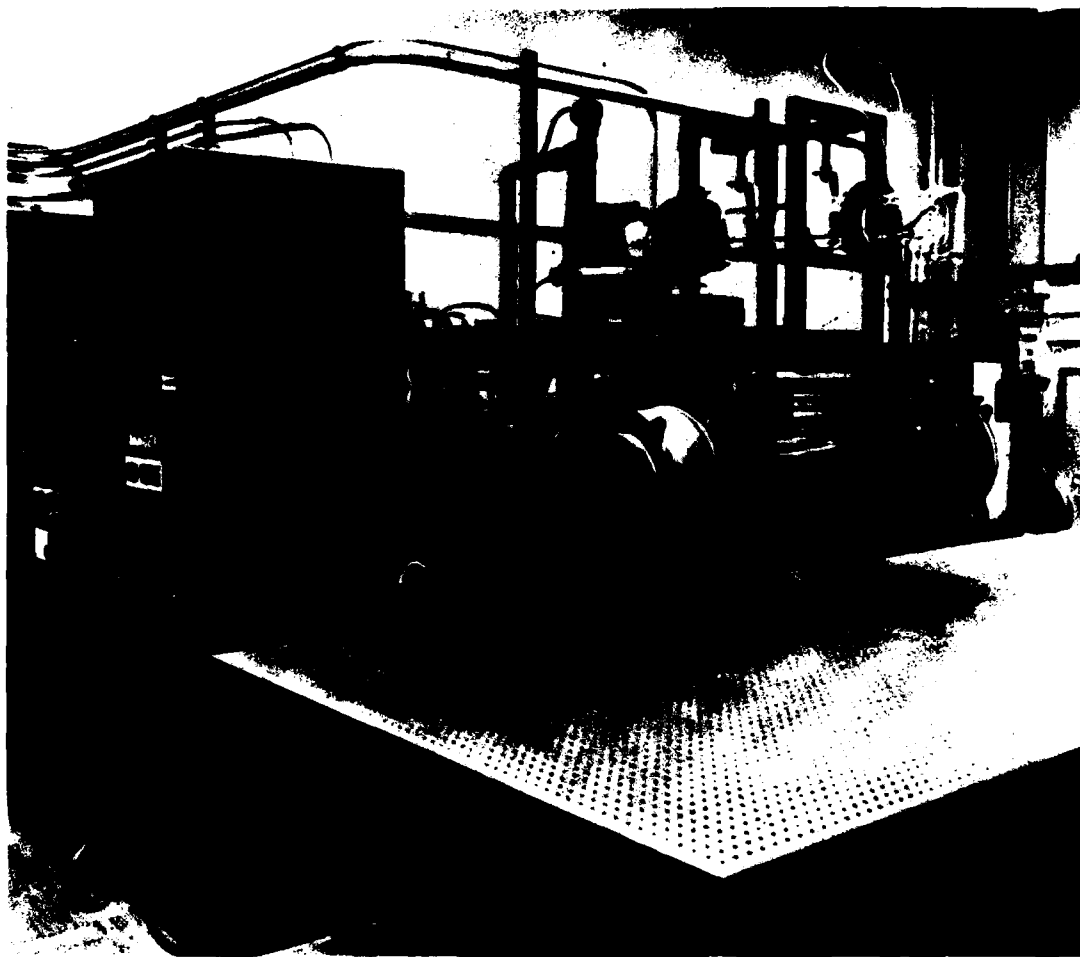Fig. 3. Schematic Diagram of Closed-Cycle CO_2 Laser Facility

Fig. 4. Photograph of Laser Facility with Optical Table

Fig. 5. Photograph of Laser Facility - Rear View that Shows Roots Blower and Refrigeration Unit.

large Roots pump with its base and mount is in the center of the photograph, the pump inlet is at the top, a water-cooled Freon refrigeration unit is at the right, and the plenum chamber is behind the unit. The Roots pump is less noisy than originally expected, and the working environment is quite acceptable. The pump vibration, which is minimal, appears to have little effect on the sensitive optical mounts of the laser resonators on the optical table.

B. GAS FLOW PARAMETERS

The physical constants for the constituent gases are provided in Table 1, and the gas flow parameters are listed in Table 2. Some of the significant characteristics of the gas mixture and flow conditions should be discussed. The gas pressure is relatively low, but the gas flow is still in the continuum regime because the mean free paths are only a few micrometers at the operating pressures. The gas flow velocity is much less than the speed of sound, except at the sonic orifices; compressibility effects are therefore negligible. Calculations and measurements have indicated that the gas friction losses in the discharge tube and the connecting pipes are also very low. The thermal conductivity of helium is high, so that even at gas pressures of a few Torr, the heat exchangers are efficient. This was also verified by experimental tests.

The gas is compressed by the Roots pump and is then expanded through 50 small holes, 1/4-in. diameter each, located around the inner wall of the inlet manifold. This procedure results in a relatively uniform flow in the discharge tube. The pressure ratio across these inlet orifices is 4.60. For a nominal operating pressure of 3.5 Torr in the discharge tube, the upstream pressure is 16 Torr. The mass flow across a sonic orifice is given by

$$\dot{m} = A^* \left[\gamma \left(\frac{2}{\gamma + 1} \right)^{\gamma+1/\gamma-1} P_o \rho_o \right]^{1/2}$$

which becomes

$$\dot{m} = A^* \left[\frac{3}{2} \left(\frac{4}{5} \right)^5 P_o \rho_o \right]^{1/2}$$

21

Table 1. Constituent Gas Constants

Gas	Molecular Weight	γ	C_p, J/g-K	Viscosity, μm (poise)	Heat Conductivity k, $W/n^2-{}^{o}C/n$
CO_2	44.011	1.304	0.8326	1.39×10^{-4}	0.0149
N_2	28.016	1.404	1.0369	1.71×10^{-4}	0.0244
He	4.003	1.660	5.233	1.86×10^{-4}	0.1438

Table 2. Summary of Gas Flow Conditions

Gas mixture	1:1:4 of CO_2:N_2:He
Average molecular weight	14.67
Effective value of γ	$\gamma = 1.50$
Sound speed of gas	$c = 481.7$ m/s
Normal operating pressure	
Discharge tube	$p_1 = 3.5$ Torr
Upstream of inlet	$p_0 = 16$ Torr
Gas velocity in discharge tube	$u = 53.3$ m/s
Mass flow	$\dot{m} = 6.02$ g/s
Volumetric flow	$uA = 2.0$ m^3/s $= 4230$ cfm

for $\gamma = 1.5$. The area of the 50 inlet holes is $A^* = 0.0015835$ m^2. The inlet gas pressure and density are $p_o = 2133.2$ newtons/m^2 and $\rho_o = 0.01378$ kg/m^3, and the mass flow is calculated to be $\dot{m} = 6.02$ g/s at 0^oC. The volumetric flow is determined from the mass flow by $\dot{m} = \rho uA$. At 3.5 Torr, $\rho = 3.0144$ g/m^3, so $uA = 2.0$ m^3/s, which corresponds to 4230 cfm. The Roots pump is rated at 6800 cfm, so there appears to be some loss in pump efficiency and perhaps some pressure drop across the finned coolers. The cross-sectional area of the discharge tube is 0.03748 m^2, so the flow velocity $u = 53.3$ m/s.

C. FLOW MEASUREMENTS

Measurements were made of the pressures, temperatures, and index of refraction changes in order to establish the flow parameters and flow uniformity. In addition, photographs were taken of the tube luminosity to determine the electrical discharge uniformity. Pressure measurements are made with capacitance manometers, which are routinely used for the determination of the tube operating pressure and upstream pressure. An operating pressure of 3.5 Torr is normally used, because near-maximum gain can be achieved without overloading the Roots pump. Thermocouples are placed at several locations around the flow circuit to monitor the performance of the coolers. It was determined that the gas temperature at the inlet manifold is usually 18 to 20^oC. The gas is heated by the electrical discharge to about 36^oC when using a nominal pulse repetition rate of 10 to 15 pulses/s. This gas is then cooled to -15^oC before it enters the inlet to the Roots pump. The gas is heated by the Roots pump to about 120^oC and is cooled to -10^oC before it enters the 6 in. diam glass pipe.

Interferometer measurements were made to determine the variation of optical path length across the tube cross section. Zygo interferometer fringe patterns for no flow and flow conditions are shown in Fig. 6. A superposition of these two patterns results in a Moire pattern that indicates clearly the optical path difference (OPD), which is also shown in Fig. 6. There is evidently a gas density change from the center to the outside of the tube that results in an OPD of 4 λ, double pass, at 6328 Å, which is the wavelength of the He:Ne laser source used in the Zygo interferometer. The OPD can be

24

TUBE
CENTER

EDGE OF
WINDOW

ZYGO
INTERFEROMETER
FIELD OF VIEW,
4-in. DIAM

OPD MAP,
UNITS OF
λ/2 FOR
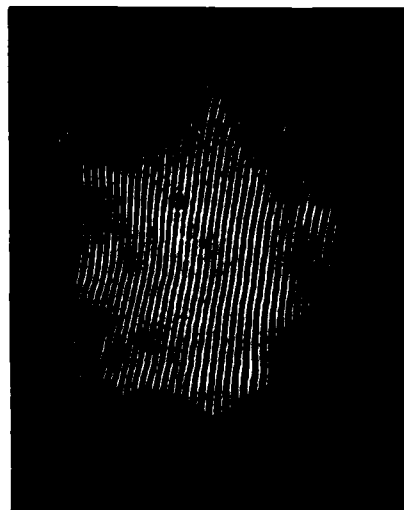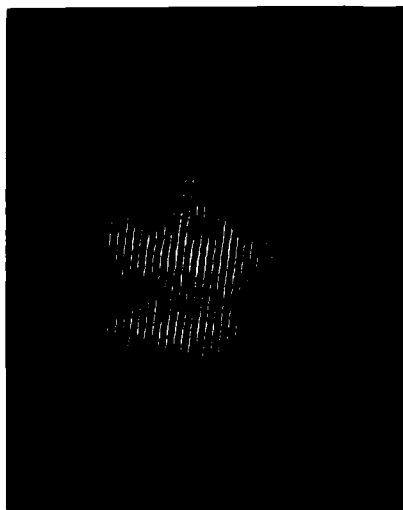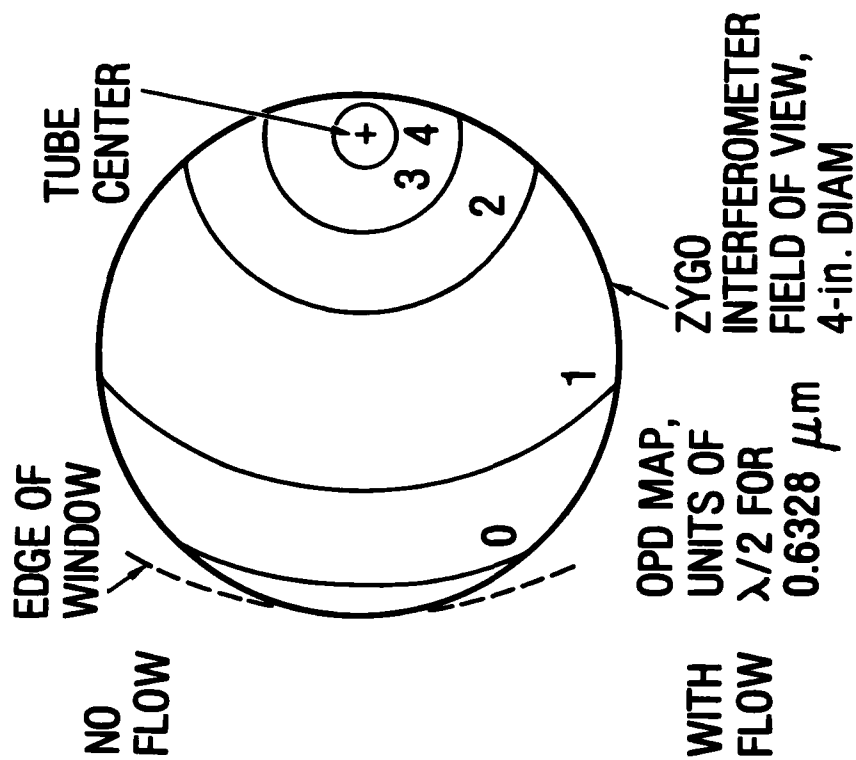0.6328 μm

NO
FLOW

WITH
FLOW

Fig. 6. Zygo Interferograms for No-Flow and Flow Conditions and Map of
Optical Path Difference between the Two Conditions

25

decomposed into a spherical component of 2 λ, which should not degrade the beam quality, and into a nonspherical component of 2 λ, double pass. The latter component amounts to an error of about $\lambda/16$, single pass, for λ = 10.6 μm. When only the outside annular region of the tube is used with the HSURIA, for example, the OPD that results from the flow is much less. Interferograms were also obtained when the current pulser was synchronized with the shutter of the Zygo interferometer, so that a single current pulse was produced when the shutter was open. There was very little change from the interferogram made with no current pulse, which means that the current pulse makes little difference in the OPD.

Photographs of the discharge luminosity taken end-on through the tube indicate a decrease of luminosity in the center of the tube. Gain measurements, described in Section V, also show a minimum at the center of the tube. When the gain medium is used for tests of annular resonators, however, the annular portion of the gain medium is very uniform.

V. ELECTRICAL DISCHARGE

A. SYSTEM SCHEMATIC

A high-voltage circuit was designed and built to supply a continuous-glow discharge current of 60 to 70 mA and a repetitive pulse current of up to 6 A with a duration of up to 2 ms and a pulse rate of up to 20 pulses/s. The pulse current amplitude, duration, and repetition rate are continuously variable. A schematic diagram of the high-voltage electrical discharge circuit is shown in Fig. 7. Two large filter capacitors, 14 µF each, are used to maintain the supply voltage to the pulser at a relatively constant value. These capacitors are charged through a 20 kohm bank of resistors and can be discharged rapidly through the same resistors by a vacuum relay. The glow discharge current is supplied directly from the power supply through a bank of 1.5 meg ballast resistors.

The high-current pulses are generated by a pair of high-voltage vacuum tubes whose grids are controlled by a separate grid bias and pulse circuit, as shown in Fig. 8. The glow discharge current and pulse current are supplied to a high-voltage bus, which connects to 12 anodes through individual ballast resistors. The cathodes are connected to a ground bus through individual ballast circuits described below. The resistors in the pulser circuit are non-inductive, and low-inductance circuit connections are used to minimize inductive effects.

B. ELECTRODE CONFIGURATION

Twelve aluminum button electrodes, 1.25 cm diameter, are mounted in a 1-in.-thick Teflon ring at each end of the 91.4-cm-long glass discharge tube. The anodes are connected to a high-voltage bus ring with 1000-ohm resistors, and the cathodes are connected to a ground bus ring with 5000-ohm resistors. These resistors were necessary to evenly distribute the glow discharge current over all 12 electrodes. The voltage drop across these 5000-ohm ballast resistors is only 30 V for the glow discharge, but for a pulse discharge current of 6 A, the voltage drop would be 2500 V. To reduce this voltage, a varistor
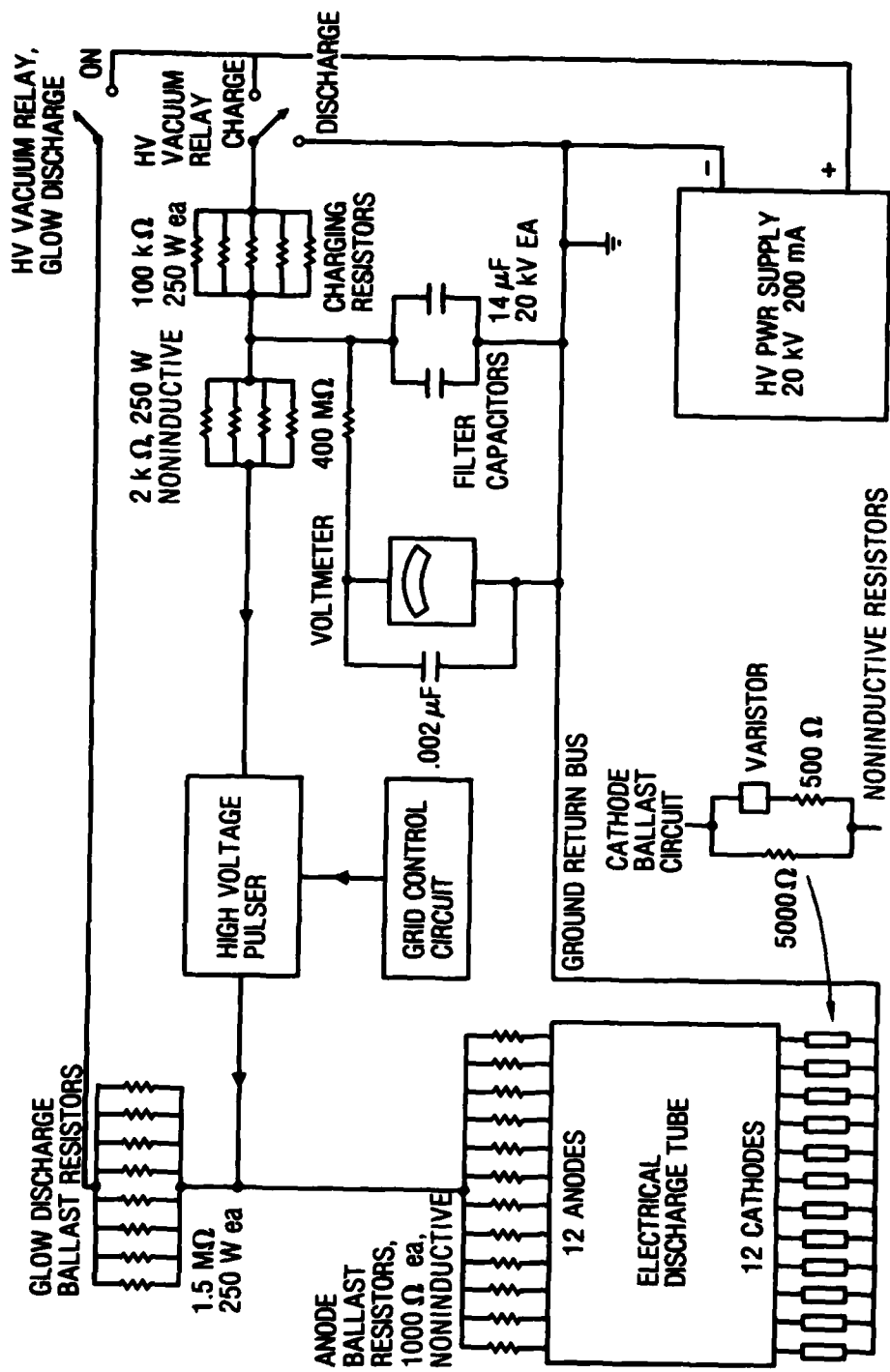
Fig. 7. Schematic Diagram of High-Voltage Electrical Discharge Circuit

28

+1350 V
POWER
SUPPLY

HV PULSE
OUTPUT

6 μF

EIMAC 8189/4PR1000A
HV TETRODES

SCREEN GRID

CONTROL GRID

CONTROL
GRID
CIRCUIT

+HV INPUT

CONTROLS FOR NEGATIVE BIAS,
PULSE DURATION PULSE
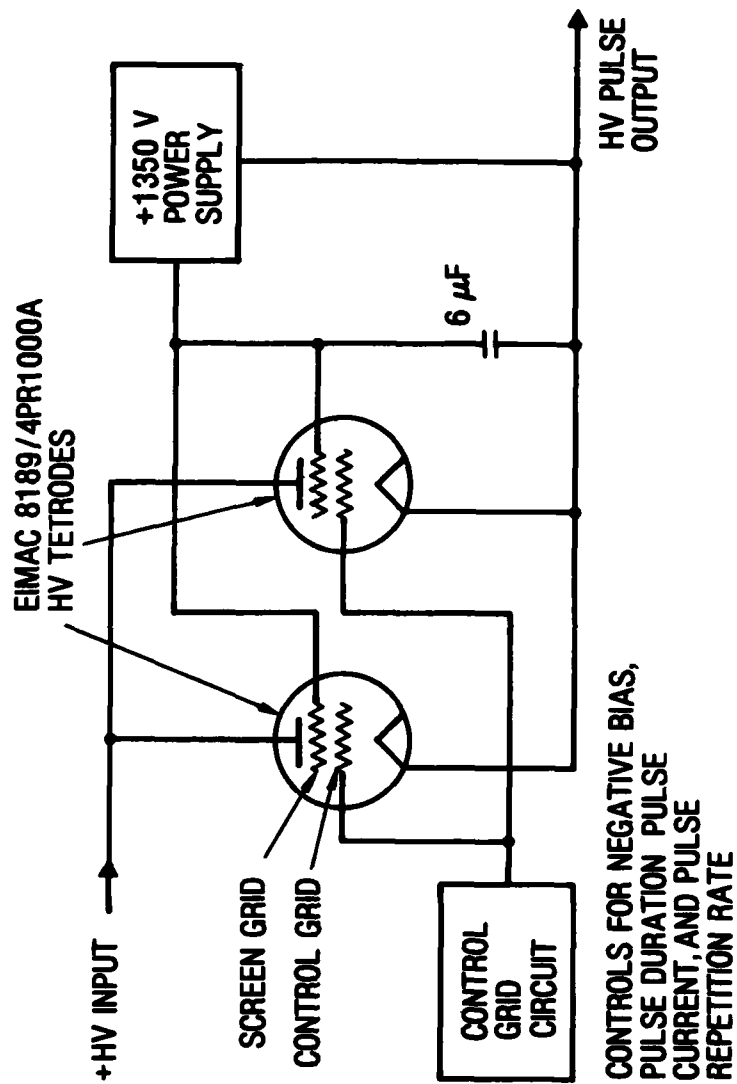CURRENT, AND PULSE
REPETITION RATE

Fig. 8. Schematic Diagram of High-Voltage Pulser Circuit

29

with a breakdown voltage of about 200 V, in series with a 500-ohm resistor, was placed across the 5000-ohm resistor. This reduces the voltage drop to about 450 V. During both the glow and pulsed discharge, all the electrodes appear to be active, and the discharge appears to be evenly distributed around the tube.

C. CURRENT AND VOLTAGE MEASUREMENTS

The pulse current is measured with a Pearson Model 411 current transformer that produces 0.1 V/A with a 10 ns rise time and very little droop during the 1 to 2 ns pulse duration. A typical current pulse is shown in Fig. 9a. The current is quite constant, except for an initial transient.

The voltage drop across the discharge tube for the cw glow discharge only was measured to be 2.43 kV for 70 nA at a gas pressure of 3.5 Torr. The transient behavior of the voltage across the tube during and after a pulse is more complex. Oscilloscope traces are shown in Fig. 9b and 9c.

A graph of this transient voltage pulse, reduced from oscilloscope data, is shown in Fig. 10. The voltage drop before the current pulse is 2.43 kV, and the gas is weakly ionized. At the start of the pulse, the voltage rises to 4.18 kV because a large current is flowing through the weakly ionized gas. As the ionization increases, the voltage decays to 3.38 kV during the 1.2-ns pulse duration. When the pulse current is cut off, the voltage across the tube suddenly drops to 0.43 kV because only the 70-nA glow-discharge current is flowing through a strongly ionized gas. The ions and electrons then slowly recombine so that an equilibrium voltage of 2.43 kV is reached for the glow discharge.

The high-voltage capacitors are partially discharged during each pulse and then charged between pulses. The voltage change ΔV is then

$$\Delta V = \frac{1}{C} \int_0^{\tau} I dt = \frac{6 \times 1.25 \times 10^{-3}}{28 \times 10^{-6}} = 268 \text{ V}$$

30

(a)   CURRENT
       TRACE

0.2 ms/div, 2.0 A/ div

(b)   VOLTAGE
       TRACE

0.2 ms/div, 2 kV/div

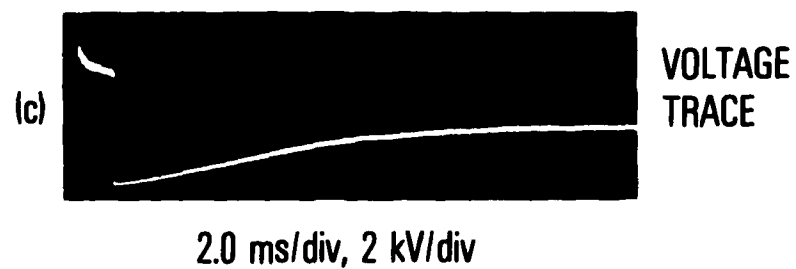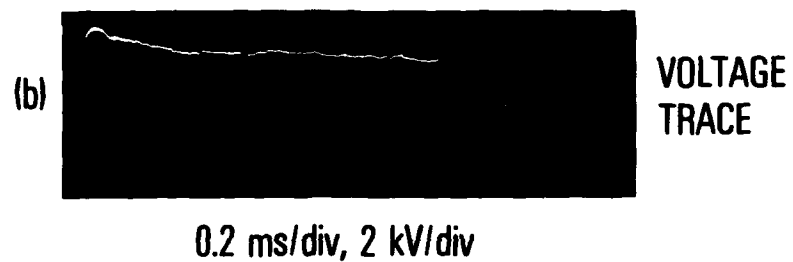(c)   VOLTAGE
       TRACE

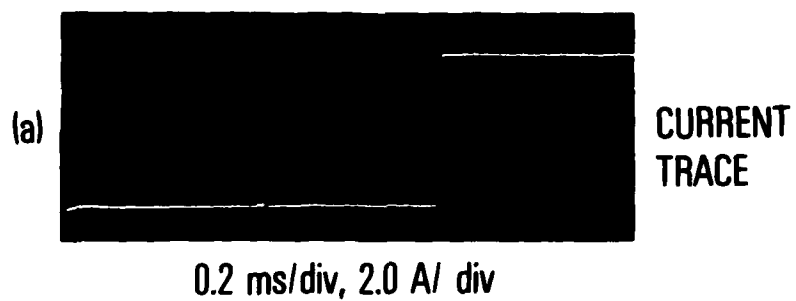2.0 ms/div, 2 kV/div

Fig. 9.   Current and Voltage across Electrical Discharge
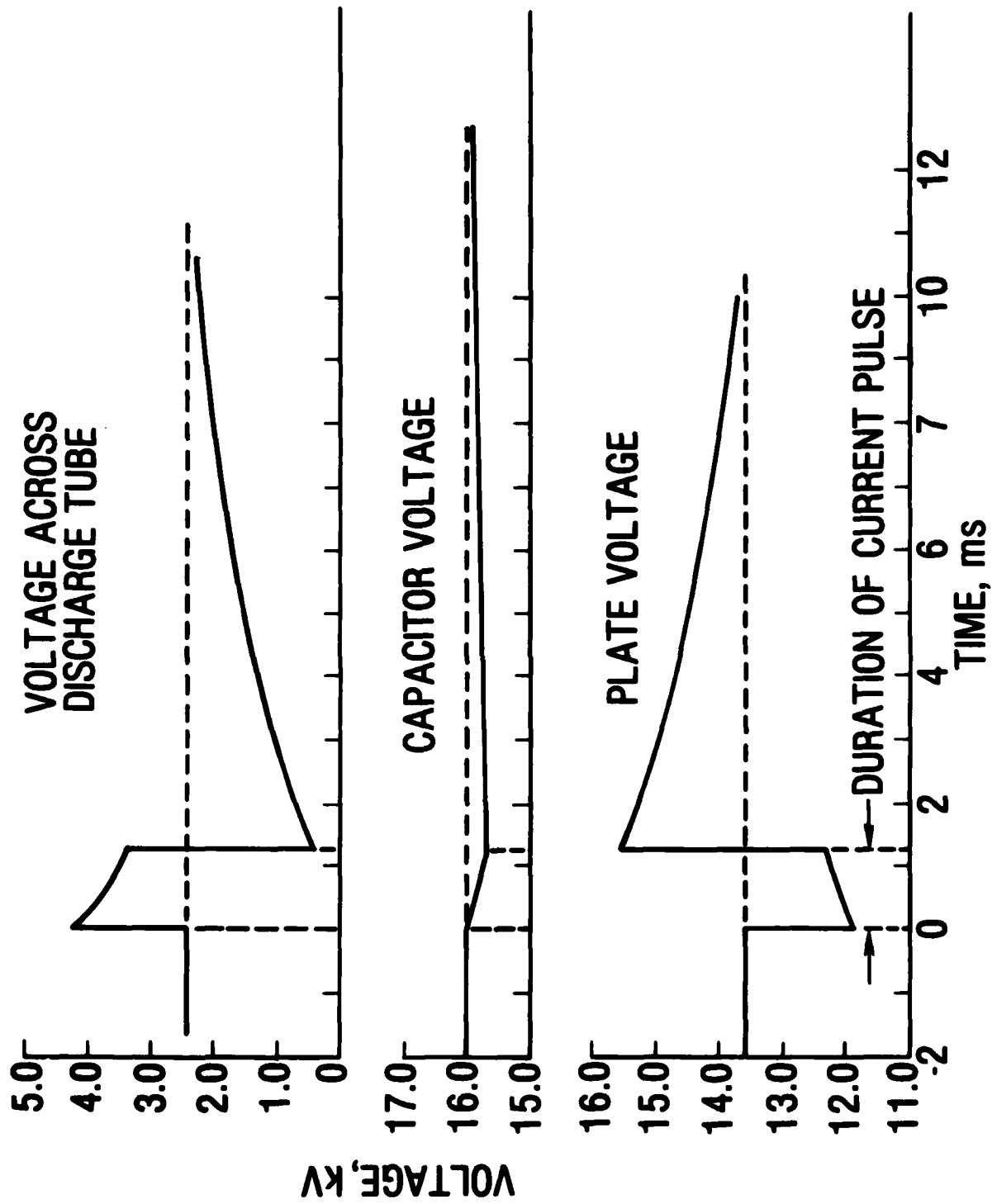   Tube

Fig. 10.   Transient Voltage across Discharge Tube. Filter Capacitors, and
Vacuum Pulser Tubes

The voltage across the high-voltage tetrodes is the capacitor voltage minus the voltage across the discharge tube, because the chassis of the high-voltage pulser is tied to the anode bus. From the previous graph of the temporal behavior of the voltage across the discharge tube, the plate voltage can be determined, also shown in Fig. 10. The plate voltage becomes 11.82 kV at the start of the pulse and then rises to 12.35 kV by the end of the pulse. For a given grid voltage, the tube current increases relatively slowly with increasing plate voltage. Therefore, the change in tube current is very small during the pulse.

VI. SYSTEM PERFORMANCE

A. GAIN MEASUREMENTS

The gain was measured with the use of a low-power, tunable Sylvania Model 950 CO_2 laser. A schematic diagram of the gain measurement optical system is shown in Fig. 11. The beam of a He:Ne laser was made colinear with the CO_2 laser beam for the purpose of optical alignment. A small fraction of the beam was directed through the electrical discharge tube through small NaCl windows. A calibration was obtained with the use of a chopper; the chopper was then set in the open position for the gain measurements. A series of several super-imposed oscilloscope traces were made during each camera exposure to obtain a good average value of the gain. Figure 12 is a typical oscilloscope photo-graph of the gain signals. The baseline is the cw laser signal I_0. The gain signal I(t) rises rapidly during the current pulse and reaches a peak value at the end of the pulse. The gain then decays to zero in a few milliseconds. The gain g(t) is given by

$$g(t) = \frac{1}{\ell} \ln \frac{I_0 + I(t)}{I_0}$$

Gain measurements were made on axis and at 1.5 and 3.0 in. off axis for a variety of conditions and for three spectral lines, P(16), P(18), and P(20).

Measurements were made for a range of pressures from 2.5 to 4.5 Torr, and the expected increase of gain with pressure was observed, as shown in Fig. 13a. The gain at 2.6 Torr is well above threshold for a resonator with M = 2, so lasing should occur at this pressure. The gain in the center of the discharge tube is somewhat lower than in the outer annulus. This is indicated by data taken at a pressure of 3.6 Torr, which are presented in Fig. 13b. It was found that the gain in the center of the tube could be increased somewhat by the use of a longer current pulse with less current, as shown in Fig. 13c.

If it were important to increase the gain on axis, the pulse duration should be set at 2.0 ms, but for tests of annular resonators, a pulse duration of 1.25 ms is optimum. The gain data shown in Fig. 13 were obtained early in
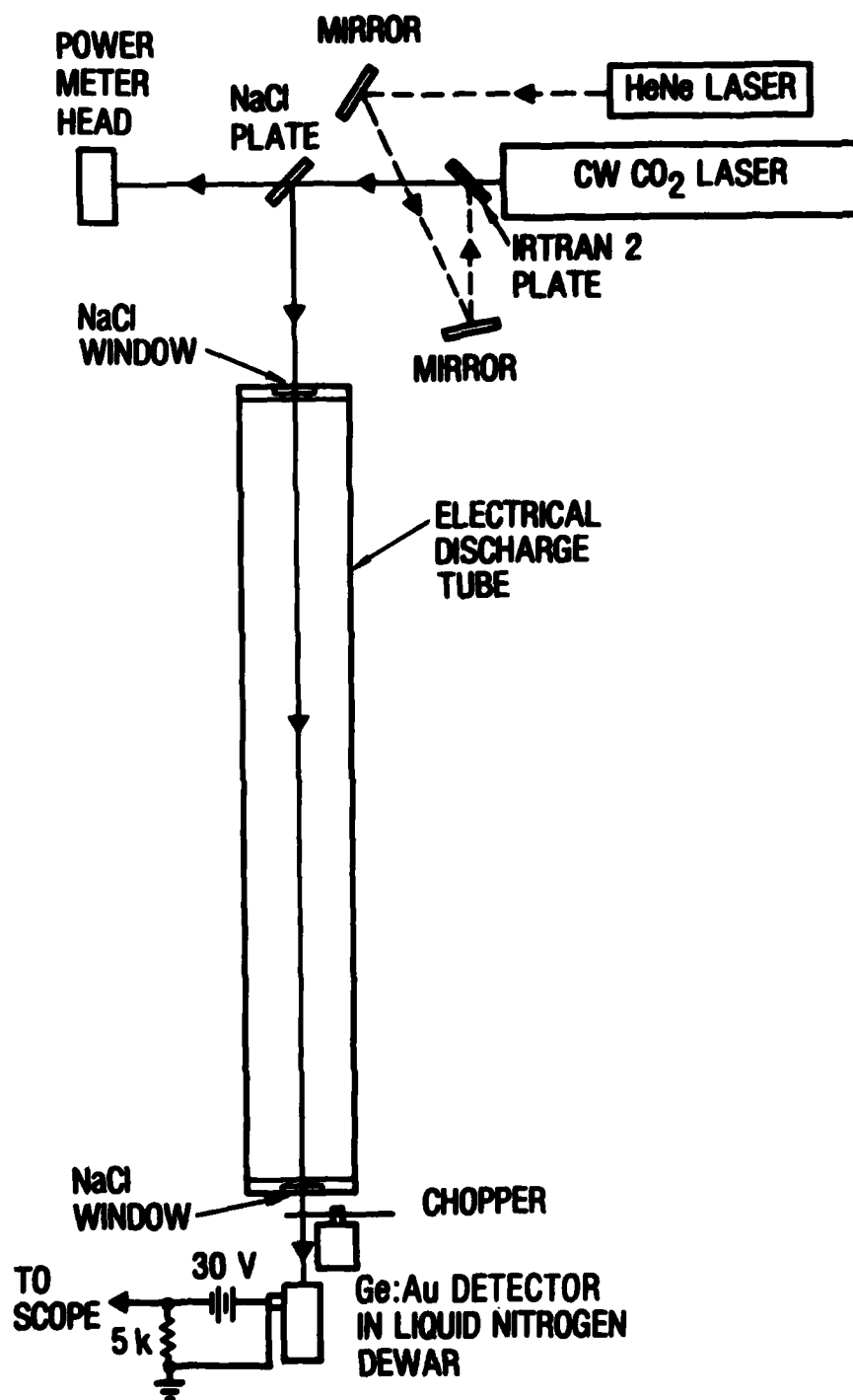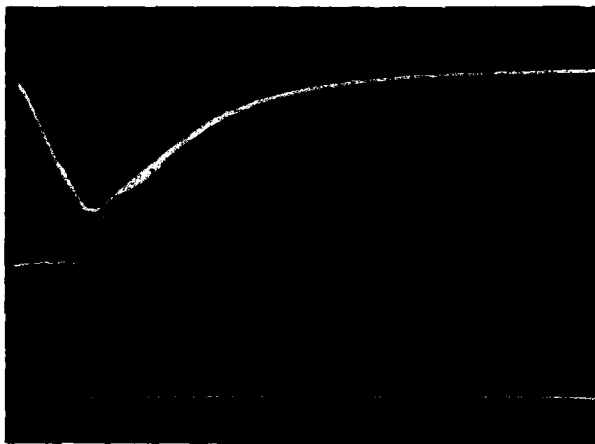
Fig. 11. Schematic Diagram of Gain Measurement System

SEVEN SUPERIMPOSED
GAIN MEASUREMENT
SIGNALS.

CURRENT TRACE,
2 A/div

1.0 ms/div SWEEP SPEED

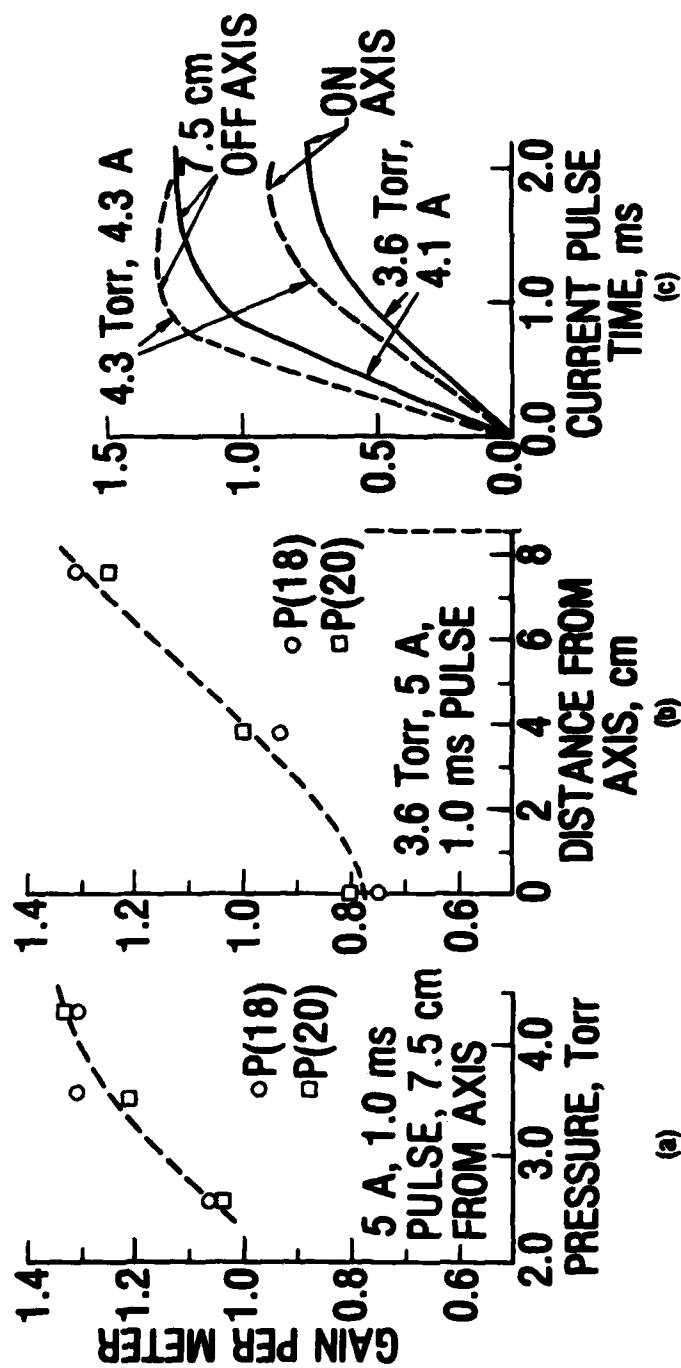Fig. 12.   Typical Gain Measurement Signals

37

Fig. 13. Gain Data

38

the test program before resonator tests were begun. Additional gain measurements were made later to obtain better spatial resolution. These measurements, which are plotted in Fig. 14, are similar to the earlier test data.

B.   PERFORMANCE WITH HSURIAs

A detailed description of the resonator tests is outside the scope of this report. However, the performance of the laser facility can be assessed by a summary of some of the results of these tests. The average laser power output for some HSURIAs has been as high as 10 W for pulse repetition rates of 10 pulses/s, which corresponds to 1.0 J/pulse. The observed near-field intensity for some resonators has been very uniform, and near-theoretical beam quality has been obtained. Therefore, the performance is not degraded by the gain medium. Lasing has been obtained at pressures of 2.5 Torr when the power output is reduced by a factor of about 2 to 3 from the nominal output at 3.5 Torr. This suggests that an even larger diameter laser facility would be feasible. An increase in diameter would require a decrease in pressure to obtain uniform electrical discharges.

In Fig. 15, laser output signals are shown from a pair of Hg:Cd:Te detectors observing the beam from a HSURIA that has a magnification of 2.2 and is operating under nominal conditions of 3.5 Torr pressure, 5.5 A, and a 1.25 ns pulse duration. Lasing is observed to switch on abruptly at 350 μs after the start of the current pulse, which is used to trigger the trace, and the output power reaches a maximum at about 900 μs. Comparison with the zero signal gain, shown in Figs. 12 and 13c, indicates that the laser output does not follow the temporal shape of the zero signal gain, but it reaches a maximum when the zero signal gain is still increasing. This behavior indicates that the medium is being partially saturated at a resonator magnification of 2.2. A spectrum analyzer has shown that the laser output is usually on the P(18), P(20), or P(22) lines of the CO_2 spectrum. The wavelength, however, was observed to shift suddenly from one line to another. At the low gas pressures, the CO_2 lines are Doppler broadened and are therefore very narrow ($\Delta v \approx 56$ MHz).

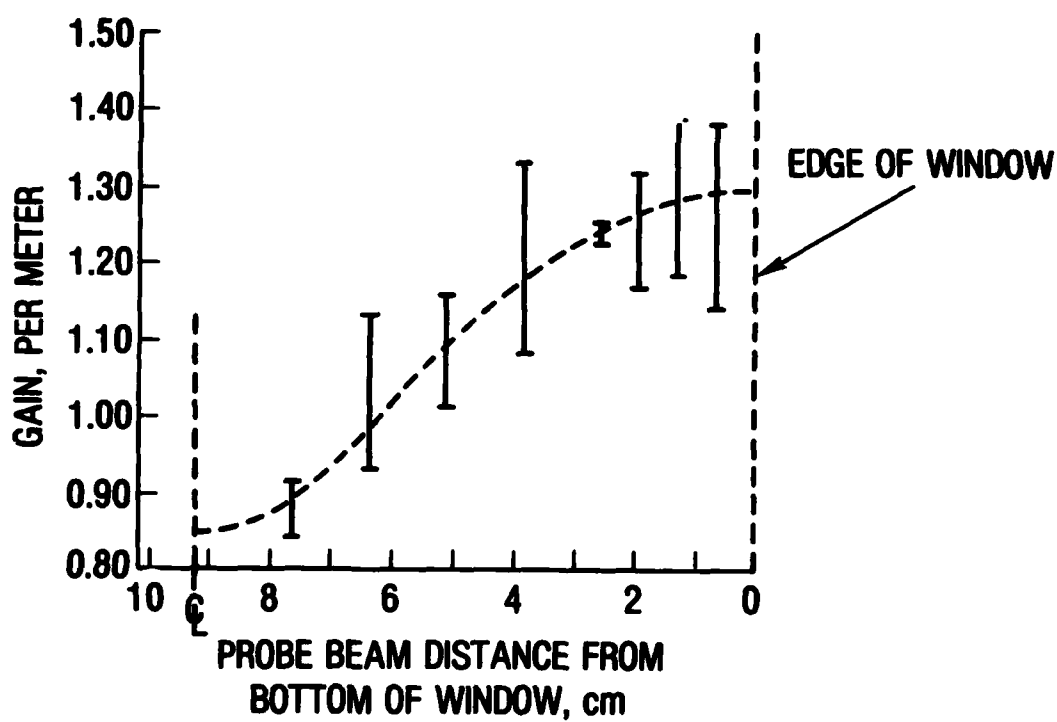P = 3.5 Torr, 6A PULSED CURRENT, 1.25 ms, P(20) SPECTRAL LINE

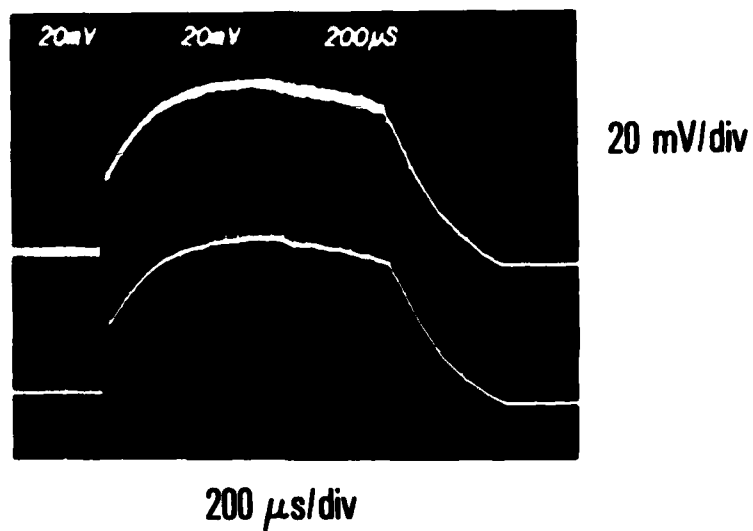Fig. 14.   Gain Measurements with Higher Spatial Resolution

20 mV/div

200 μs/div

Fig. 15. Laser Output Signal

41

The CO_2 lines at these pressures are comparable to the longitudinal mode spacing of a typical resonator. Small changes in cavity length can therefore cause the spectral output to change, because the laser will always operate at the highest gain consistent with the allowed longitudinal mode frequencies.

VII. SUMMARY

The closed-cycle CO_2 laser facility has satisfied all of the original
requirements discussed in Section II. (1) The large aperture permits the
testing of resonators at large equivalent Fresnel numbers. (2) The discharge
is uniform, and the gas flow does not introduce appreciable inhomogeneities
that could degrade the beam quality. (3) The gain is adequate for the testing
of unstable resonators at magnifications of greater than 2.0, with good gain
saturation. (4) The facility can be operated for long periods of time, and
the effects of mirror adjustments can be observed in real time. (5) Although
the instantaneous power is as large as 1 kW, the duty cycle is less than 2%,
so the average power is sufficiently low that thermal distortion of the
mirrors is no problem. (6) The system thus far has been very reliable with
minimal down time caused by equipment failures.

LABORATORY OPERATIONS

The Laboratory Operations of The Aerospace Corporation is conducting experimental and theoretical investigations necessary for the evaluation and application of scientific advances to new military concepts and systems. Versatility and flexibility have been developed to a high degree by the laboratory personnel in dealing with the many problems encountered in the Nation's rapidly developing space systems. Expertise in the latest scientific developments is vital to the accomplishment of tasks related to these problems. The laboratories that contribute to this research are:

Aerophysics Laboratory: Aerodynamics; fluid dynamics; plasmadynamics; chemical kinetics; engineering mechanics; flight dynamics; heat transfer; high-power gas lasers, continuous and pulsed, IR, visible, UV; laser physics; laser resonator optics; laser effects and countermeasures.

Chemistry and Physics Laboratory: Atmospheric reactions and optical backgrounds; radiative transfer and atmospheric transmission; thermal and state-specific reaction rates in rocket plumes; chemical thermodynamics and propulsion chemistry; laser isotope separation; chemistry and physics of particles; space environmental and contamination effects on spacecraft materials; lubrication; surface chemistry of insulators and conductors; cathode materials; sensor materials and sensor optics; applied laser spectroscopy; atomic frequency standards; pollution and toxic materials monitoring.

Electronics Research Laboratory: Electromagnetic theory and propagation phenomena; microwave and semiconductor devices and integrated circuits; quantum electronics, lasers, and electro-optics; communication sciences, applied electronics, superconducting and electronic device physics; millimeter-wave and far-infrared technology.

Materials Sciences Laboratory: Development of new materials; composite materials; graphite and ceramics; polymeric materials; weapons effects and hardened materials; materials for electronic devices; dimensionally stable materials; chemical and structural analyses; stress corrosion; fatigue of metals.

Space Sciences Laboratory: Atmospheric and ionospheric physics, radiation from the atmosphere, density and composition of the atmosphere, aurorae and airglow; magnetospheric physics, cosmic rays, generation and propagation of plasma waves in the magnetosphere; solar physics, x-ray astronomy; the effects of nuclear explosions, magnetic storms, and solar activity on the earth's atmosphere, ionosphere, and magnetosphere; the effects of optical, electromagnetic, and particulate radiations in space on space systems.